

COMMISSIONING AND EARLY OPERATION FOR THE NSLS-II BOOSTER RF SYSTEM*

C. Marques[†], J. Cupolo, P. Davila, F. Gao, A.Goel[‡], B. Holub, J. Kulpin, K. McDonald, J. Oliva, J. Papu, G. Ramirez, J. Rose, R. Sikora, C. Sorrentino, N. Towne, NSLS-II, BNL, Upton, NY 11973, USA

Abstract

The National Synchrotron Light Source II (NSLS-II) at Brookhaven National Laboratory (BNL) is a third generation 3GeV, 500mA synchrotron light source [1]. We discuss the booster synchrotron RF system responsible for providing power to accelerate an electron beam from 200MeV to 3GeV. The RF system design and construction are complete and is currently in the operational phase of the NSLS-II project. Preliminary operational data is also discussed.

INTRODUCTION

The booster synchrotron NSLS-II RF system is designed to efficiently accelerate a range of bunches from 0.5nC in single bunch mode up to 15nC in multi-bunch mode injected from the linac at 200MeV to the final acceptance energy of the storage ring of 3GeV once every second. The performance goals for the booster are derived from the beam acceptance requirements for the storage ring including an RF acceptance of 0.85% [1].

The booster RF system can be divided into five subsystems namely a 500MHz 7-Cell PETRA-like cavity, a 500MHz transmitter using a 90kW Inductive Output Tube (IOT), a 38kV/4A Pulse Step Modulated High Voltage Power Supply (HVPS), a Cavity Field Controller (CFC) and a high power circulator. Some relevant machine parameters are listed in Table 1 while the layout for the booster RF system is shown in Figure 1.

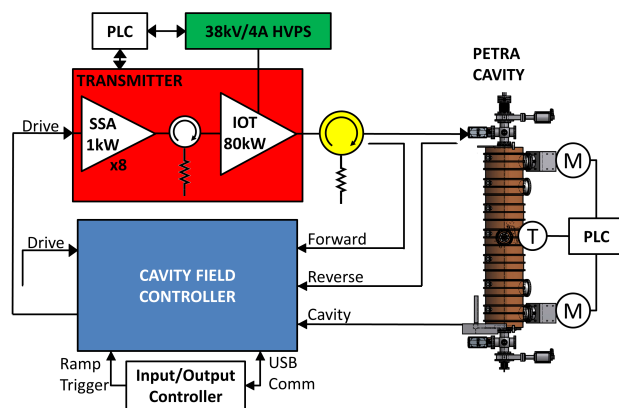


Figure 1: Simplified block diagram of the booster RF system.

* Work supported by the U.S. Department of Energy, Office of Science, Office of Basic Energy Sciences, under Contract No. DE-SC0012704.

[†] cmarques@bnl.gov [‡] Now at Argonne National Laboratory

Table 1: The NSLS-II Booster RF Parameters

Parameter	Value	Units
Frequency	499.68	MHz
Harmonic	264	
Bunch Train Charge	≤ 15	nC
Loss per turn @ 3GeV	625	keV
Gap Voltage @ Injection	200	kV
Gap Voltage @ Extraction	1200	kV
Injection Energy	200	MeV
Extraction Energy	3	GeV
RF Acceptance @ Extraction	0.85	%
Momentum Compaction	.0072	
Ramp Repetition Rate	1	Hz
Cavity Q_L	10^4	
Cavity Shunt Impedence	23	M Ω
HVPS Switching Frequency	93.75	kHz
HVPS Switching Modules	60	

SUB-SYSTEMS

Digital CFC

The Field Programmable Gate Array (FPGA) based CFC was developed as a common hardware platform for all NSLS-II RF systems and offers excellent versatility. A more detailed description of the CFC and the clock generating subsystem responsible for the FPGA clock, up/down conversions and timing can be found elsewhere [2, 3]. The booster CFC outputs a ramped RF waveform established by the host Input/Output Controller once a timing signal is initiated. The CFC uses a feedback control loop to stabilize the cavity field and phase throughout the ramp cycle.

Booster Transmitter

The 500MHz 90kW IOT is used to power the PETRA-like cavity. The cavity produces a ramped accelerating voltage from 200kV to 1200kV required for the acceleration from 200MeV to 3GeV. The measured output power of the IOT at extraction for a 3GeV acceleration was 47kW and is determined by the copper losses, beam loading and any external load. At peak operating levels the efficiency was measured to be 50%. The spectrum from the booster transmitter can be seen in Figure 2. The IOT is assembled on a cart which includes a focusing coil and input/output circuits. This modular approach allows switching out a tube assembly in about two hours. The transmitter is controlled via a Programmable Logic Controller (PLC) which communicates with the NSLS-II Experimental Physics and Industrial

Control Systems (EPICS) to ensure proper operation and shutdown in the event of an interlock fault.

Thomson HVPS

The 38kV/4A Power Supply uses a pulse step modulation (PSM) algorithm on sixty switching modules to supply power to the booster transmitter. The modular nature of the PSM system facilitates quick maintenance and repairs thereby increasing system availability. However coincidence with the synchrotron oscillation frequency (18-22kHz) and the harmonics and sub-harmonics of the HVPS switching frequency is possible. To avoid this detrimental coupling, the HVPS switching frequency parameter can be adjusted using a terminal program. By adjusting the switching frequency its harmonics and sub-harmonics are placed about the synchrotron oscillation frequency. Additionally subharmonic frequency lines produced by the switching modules as well as mains harmonics are below -70dBc. The HVPS system is tolerant of failed switching modules. The switching logic redistributes the load across the operational modules albeit at the cost of a minor drop in output voltage. The suggested software limit on operation with failed modules is five. It is possible to reprogram the unit to operate with additional failed units but doing so reduces the HV output and increases the harmonic content in the RF output.

7-Cell PETRA-like Cavity

The 500MHz 7-Cell copper cavity was originally designed for the Positron-Elektron-Tandem-Ring-Anlage (PETRA) facility in Deutsches Elektronen-Synchrotron (DESY) [4]. The cavity includes two plunger style tuners controlled by a PLC to adjust the frequency and both move synchronously to preserve field flatness during operation. The tuner assembly was retrofitted with Linear Variable Differential Transformers (LVDTs) to eliminate backlash from the geared tuner position sensor and increase position resolution. A polynomial function of a PT100 temperature reading versus LVDT voltage output controls the cavity tuner position via a PLC. This temperature sensor is thermal epoxied on the PETRA cavity and can be seen on the schematic in Figure 1. The temperature dependent LVDT position programmed into the PLC accounts for the beam loading at extraction and minimizes the reflected power in the presence of temperature drifts by maintaining a cavity frequency offset from the 499.68MHz operating frequency; preserving the reference phase for Robinson stability [5].

The calculated critical coupling factor to match the transmitter to the cavity at nominal beam loading at extraction is 1.6. An overcoupled coupling factor of 1.8 was chosen to make the RF system less sensitive to beam loading effects. The original coaxial to waveguide transition was replaced by a cheaper, more compact and easier to install shorted coaxial T feed.

Circulator

The 500MHz ± 2 MHz 100kW CW circulator is used as an isolator for the outgoing RF and beam induced power. The

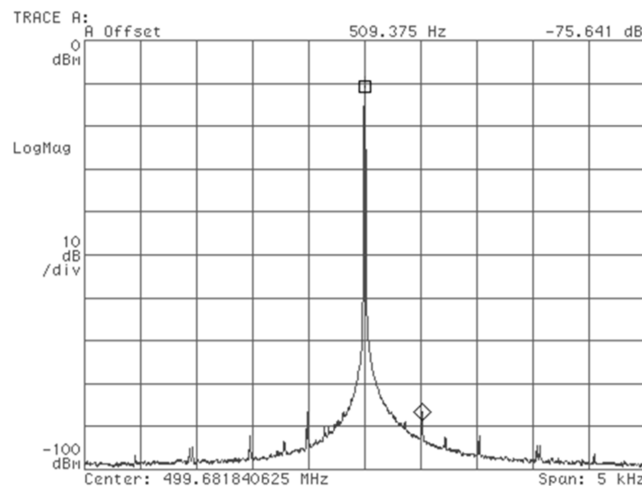


Figure 2: Averaged IOT spectrum with feedback, taken with an RBW of 10Hz.

maximum calculated beam power at extraction and the maximum RF power required for the 3GeV booster is 19.2kW (15nC = 28mA) and 45kW respectively or 64.2kW combined. A test was performed by placing a short across the output port of the circulator at 80kW where all the power was successfully dumped to the RF load. The RF load is a dry-type ferrite absorber capable of withstanding 120kW CW. Both the circulator and the RF Load use WR1800 waveguide which is converted to 6 1/8 inch 50Ω coaxial transmission lines to the transmitter and cavity.

INITIAL RESULTS

Typical data of the booster injection and extraction performance taken from the “Booster Status Page” on EPICS during normal operations can be seen in Figure 3. The RF digital waveform from the CFC resembles the dipole power supply cycle [6]. Using the booster DCCT, the injected and ramped current can be monitored during the ramp process. The beam is extracted at the maximum field of the ramp around 392ms into the NSLS-II storage ring. The injection vs. extraction beam current yields an efficiency of 97% and since entering the operational phase the booster efficiency has remained > 90% on average.

Fault Statistics

All major alarms are sent to the NSLS-II control room through the Best Ever Alarm System Toolkit (BEAST). Some of the top accumulated alarms from the booster RF which have been registered by the BEAST can be seen in Figure 4. These faults were data-logged during commissioning and operations and are registered regardless of how they are initialized including testing, software/hardware glitches and actual trips provided the BEAST is armed. These faults can also be filtered given a particular criteria for example if the fault was during a maintenance period or if the fault was a “major” alarm.

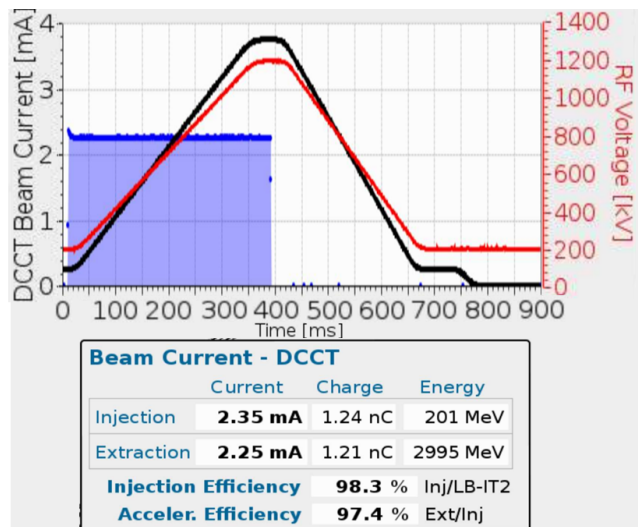


Figure 3: Preliminary injection and extraction data for the booster system. The blue curve represents the DC current transformer (DCCT) which is proportional to the beam current, red represents the RF cavity voltage and the black line represents the booster dipole current, all as a function of time.

The top accumulated fault, the Personnel Protection System (PPS) trip is initiated whenever a safety interlock is breached throughout the NSLS-II facility or by false alarms described above. Once initiated the PPS trip opens a main contactor which disconnects the mains from the HVPS. In the original design of the booster RF system, a PLC was used to switch off the transmitter before opening the contactors. However there was a possibility of opening the contactor while the HVPS was still under load. A fast interlock was added to drop the HVPS current before opening the contactor in the event of a PPS trip and potentially preventing any damage to the HVPS.

Not shown in Figure 4 are the many false arc alarms triggered by the spare arc detection channels of the arc detection module. There were approximately 200 false alarms for each spare channel which have since been removed from the alarm supervision. These trips indicate either a malfunction within the arc detection box, a false trip due to other sources of radiation for example cosmic rays, noise, etc. These false trips are probably not localized to the spare arc detection channels and can lead to false alarms for the active channels monitoring the RF system including the RF load arc trips. A voting scheme is under investigation to rectify this issue.

The booster RF has tripped 526 “major” alarms during operations since September 1, 2014 until April 14, 2015. These accumulated trips do not include trips which occurred during maintenance or shutdown periods and these alarms would disable the booster RF until a reset of the fault was executed. A full recovery of the booster RF system after a trip typically takes about 10 minutes aside from four instances. The majority of these four instances involved a transient from the mains. This yields a booster RF reliability of 98% and

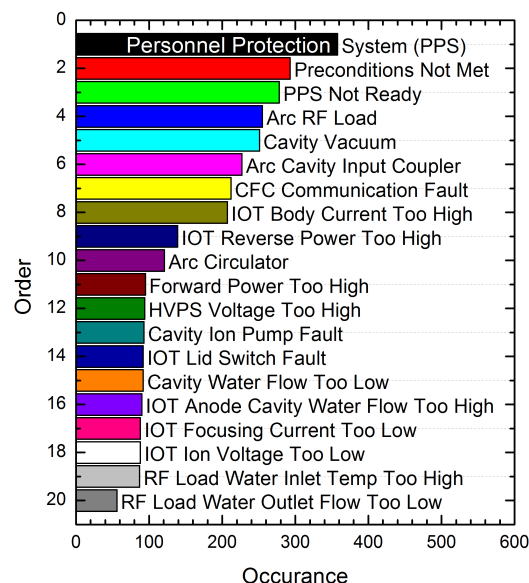


Figure 4: Top 20 accumulated Booster RF trips since entering the NSLS-II since September 1, 2014 until April 14, 2015.

is improving after each resolution of software and hardware vulnerabilities.

SUMMARY

The general requirements in terms of RF power and phase stability for the booster have been met. As of 2011 the booster RF system has been operational with excellent reliability and performance.

ACKNOWLEDGMENT

The authors wish to acknowledge the help and discussions of J. Tagger, S. Buda, E. Moeri and T. Shaftan. We appreciate our colleagues at Canadian Light Source (CLS) for allowing us to successfully field test the CFC on the CLS booster RF system. In addition the continuous support from the NSLS-II Controls and Utilities groups.

REFERENCES

- [1] NSLS-II preliminary design report, <http://www.bnl.gov/nsls2/project/PDR/>.
- [2] J. Rose *et al.*, “NSLS-II Radio Frequency Systems”, in *Proc. IPAC’15*, Richmond, VA, USA, May 2015, paper TUPMA052, these proceedings.
- [3] B. Holub *et al.*, “NSLS-II Digital RF Controller Logic and Applications”, in *Proc. IPAC’15*, Richmond, VA, USA, May 2015, paper MOPTY038, these proceedings.
- [4] H. Gerke, H.P. Scholz, M. Sommerfeld, and A. Zolfaghari, “Das PETRA Cavity”, DESY PET-77/08.
- [5] K. Robinson, “Stability of Beam in RF System”, CEAL-1010, 1964.
- [6] T. Shaftan and J. Rose, “Specifications on the RF ramp for the NSLS-II booster”, NSLS-II Technical Note 107, 3 June 2013.